

Segregation of object and background motion in the retina

Bence P. Ölveczky*†, Stephen A. Baccus‡ & Markus Meister‡

* Division of Health Sciences and Technology, Massachusetts Institute of Technology, 77 Massachusetts Avenue, Cambridge, Massachusetts 02138, USA

† Program in Neuroscience, Harvard University, 220 Longwood Avenue, Boston, Massachusetts 02115, USA

‡ Department of Molecular and Cellular Biology, Harvard University, 16 Divinity Avenue, Cambridge, Massachusetts 02138, USA

An important task in vision is to detect objects moving within a stationary scene. During normal viewing this is complicated by the presence of eye movements that continually scan the image across the retina, even during fixation. To detect moving objects, the brain must distinguish local motion within the scene from the global retinal image drift due to fixational eye movements. We have found that this process begins in the retina: a subset of retinal ganglion cells responds to motion in the receptive field centre, but only if the wider surround moves with a different trajectory. This selectivity for differential motion is independent of direction, and can be explained by a model of retinal circuitry that invokes pooling over nonlinear interneurons. The suppression by global image motion is probably mediated by polyaxonal, wide-field amacrine cells with transient responses. We show how a population of ganglion cells selective for differential motion can rapidly flag moving objects, and even segregate multiple moving objects.

Movements of the eye are a fundamental component of vision, as they directly influence the stimulus falling on the retina. There are two main types of eye movement: the large and rapid saccades or pursuit movements by which we redirect our gaze, and the smaller fixational eye movements that occur between saccades^{1,2}. Whereas ballistic gaze-shifting eye movements suppress vision³, small fixational eye movements are essential for seeing: if the retinal image is stabilized, visual perception fades within a tenth of a second⁴.

During fixation, the retinal image drifts over about 0.5° of visual angle, or about 60 cone receptive fields, at an average speed of approximately 0.5 degrees s⁻¹, and any processing of visual information must occur on the background of this drifting motion⁵.

Similar eye movements occur in other animals, including salamander⁶ and rabbit⁷. Despite their importance to vision, the effect of these eye movements on retinal function has received rather limited attention.

Given the presence of continuous eye movements, the fundamental task of detecting object motion within a scene becomes a significant computational problem. The task is not simply to detect motion on the retina; rather, the visual system must discriminate between local motion patterns specific to an object and global motion induced by fixational eye movements⁸. Humans perceive this task as effortless: movements anywhere within a scene immediately ‘pop-out’ and attract our attention⁹, even if their velocity and amplitude is only a fraction of the image motion caused by

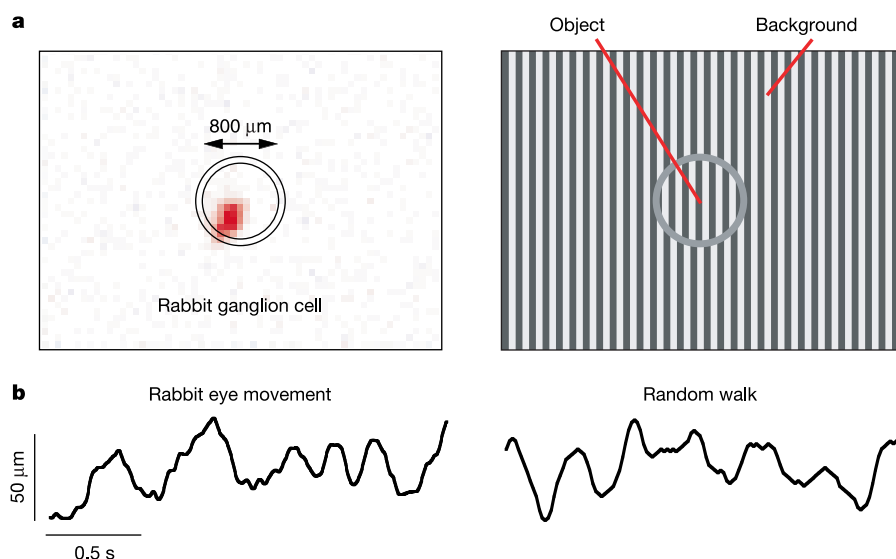


Figure 1 Simulating local object motion on the retina in the presence of fixational eye movements. **a**, Receptive field profile of a rabbit ON Brisk Transient retinal ganglion cell (left; see Methods). A stripe grating representing an object was projected in and around the cell's receptive field centre, while the remainder of the retina was presented with a background grating (right). **b**, Trajectory of vertical fixational eye movements in an unrestrained rabbit, acquired using a scleral search coil⁷ (left). The right panel shows a sample of the random walk trajectory used to jitter the gratings.

fixational eye movements¹⁰. A neuron that subserves this function should respond to local motion on the retina, but only if the motion trajectory differs from that in a large surrounding region. Neurons capable of such computations have been described in the visual cortex^{11,12} and superior colliculus^{13,14} of mammals, and also in the optic tectum of birds¹⁵. However, given that the fixational eye movements in the two eyes differ¹⁶, extraction of object motion probably happens before the visual pathways from the two eyes merge. Here we show that the segregation of object motion and image motion induced by eye movements happens in the retina.

The retina senses differential motion

We recorded the spike trains of ganglion cells in the isolated retina of salamander and rabbit. The stimulus display was divided into a small ‘object’ region overlying the receptive field centre of the ganglion cell and a surrounding large ‘background’ region covering the rest of the retina (Fig. 1a). Both object and background were given a visual texture by a simple stripe grating. The background grating jittered laterally with a random walk trajectory, similar to that of fixational eye movements (Fig. 1b). The object grating also jittered in a random walk with the same statistics, either coherently with the background, or incoherently with a different trajectory. The coherent condition simulated the global image motion on the

retina that results when viewing a stationary scene in the presence of eye movements only (‘Eye Only’ condition). The incoherent condition simulated, in addition, local motion of an object within that scene (‘Eye + Object’ condition).

In both the salamander and rabbit retina we found ganglion cells that were highly selective for motion within the scene (Fig. 2): these neurons responded vigorously to the Eye + Object condition (Fig. 2a), but were almost completely suppressed under the Eye Only condition (Fig. 2b), even though their receptive field centres experienced the same stimulus under both conditions. When the background region was uniformly grey (‘Object Only’, Fig. 2c), the responses were similar to the Eye + Object condition (Fig. 2a), indicating that an incoherently moving background has little effect on the centre response. Whereas the stimulus condition in Fig. 2a simulated an object jittering within the scene, a steady drift of the object relative to the background also elicited reliable responses (‘Eye + Object Drift’, Fig. 2d).

As these ganglion cells are selective for local object motion over global motion, we will refer to them as OMS (object motion sensitive) cells, noting that this class comprises several recognized cell types (for example, ‘ON Brisk Transient’ cells and ‘ON-OFF Direction Selective’ cells in rabbit, and ‘Fast OFF’ cells in salamander; Fig. 2e). Both retinas contain other cell types that show much

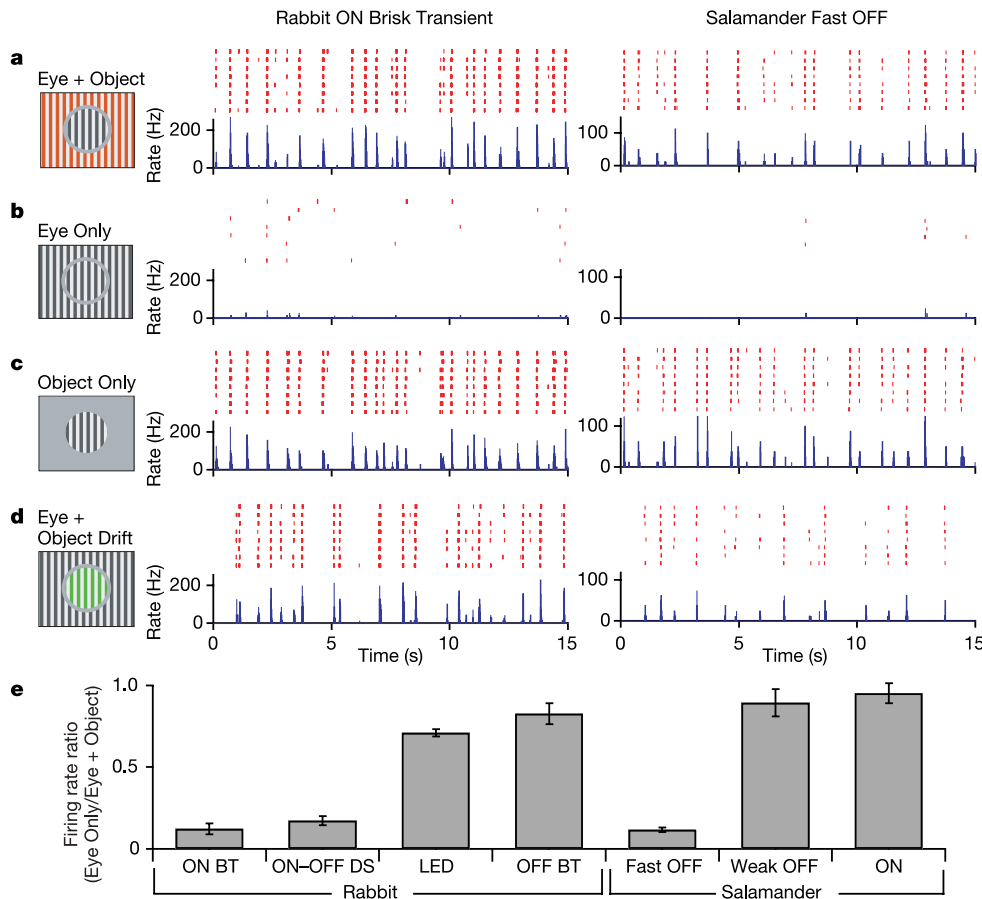


Figure 2 Certain retinal ganglion cells are selective for object motion. **a–d**, Responses to 15 s of jitter from a rabbit ON Brisk Transient cell and a salamander Fast OFF cell. Each panel shows a raster plot with spikes on eight identical stimulus trials (top) and a peri-stimulus time histogram of the firing rate averaged over all trials (bottom). The stimulus conditions are: Eye + Object (**a**), object and background gratings jittered incoherently; Eye Only (**b**), object and background jittered coherently with same trajectory as the object in **a**; Object Only (**c**), object jittered as in **a**, background grey; Eye + Object Drift (**d**),

object and background jittered as in **b** with a steady drift ($450 \mu\text{m s}^{-1}$) added to the object region. **e**, Ratio of firing rates in the coherent (**b**) and incoherent (**a**) motion condition. Data from 6 ON Brisk Transient (ON BT) cells, 11 ON-OFF Direction Selective (ON-OFF DS) cells, 5 Local Edge Detector (LED) cells, and 7 OFF Brisk Transient (OFF BT) cells in two rabbit retinas; 41 Fast OFF cells, 8 Weak OFF cells and 8 ON cells in nine salamander retinas.

smaller, if any, difference between the coherent and incoherent motion conditions (for example, 'OFF Brisk Transient' cells in rabbit and 'ON' cells in salamander, Fig. 2e). Thus, the selectivity for object motion may be a special feature of a few of the parallel pathways that convey retinal output to the brain.

Mechanism of suppression from coherent motion

OMS ganglion cells are excited by motion in or near the receptive field centre, but are suppressed if the same image motion extends over the wider surround. We measured the extent of these antagonistic regions by gradually increasing the size of the object, while keeping the trajectories in the object and background regions different (Fig. 3a). For salamander Fast OFF cells, the firing rate increased up to an object radius of approximately 250 μm : this is the extent of the region excited by grating motion and corresponds very well to the classic receptive field centre as measured by flashing spots of increasing size (Fig. 3b). As the object grew in size, it began to invade the suppressive surround region, and the response gradually decreased out to radii of about 1,000 μm . Thus, the suppressive effect of coherent motion extends over at least 1 mm on the retina. Applying strychnine largely blocked the antagonistic effect of coherent surround motion, suggesting that it is caused by long-range glycine-mediated inhibition, presumably from wide-field amacrine cells¹⁷.

Ganglion cells can be suppressed by peripheral motion^{18–20}. However, this alone does not explain our findings, as the amount of motion in the background region was identical for both the Eye + Object and the Eye Only conditions, and for all the stimuli in Fig. 3a. As seen in Fig. 2c, the OMS cells respond to a jittering object over the receptive field centre with brief bursts of spikes that are precisely timed to the motion trajectory. We hypothesized that inhibition from peripheral motion arrives in similar brief pulses

that have the same dependence on the motion trajectory as the excitatory events from the centre (Fig. 4a). Under stimulation with coherent motion, the peripheral inhibition would coincide with the excitation from the centre and suppress the cell's response. In response to object motion, when the object and background regions jitter incoherently, inhibition would arrive with random timing

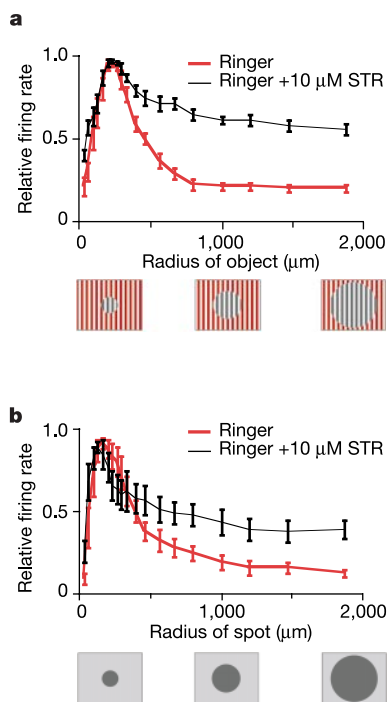


Figure 3 Spatial interactions that produce the sensitivity to object motion. **a**, Relative firing rate of salamander Fast OFF cells ($n = 5$) as a function of object size in the Eye + Object condition. **b**, Relative firing rate of the same cells to a 1-Hz flashing spot of increasing size. The black trace shows the effect of 10 μM strychnine (STR). Firing rates were averaged over 2 min of stimulation and normalized to the maximum firing rate of each cell.

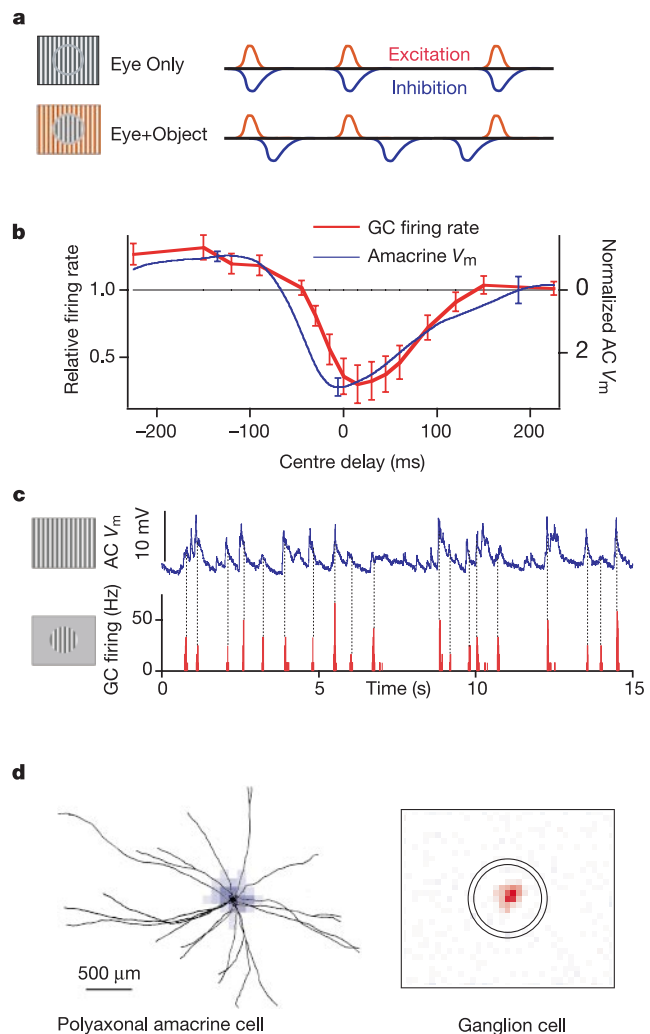


Figure 4 Transient excitation and inhibition are synchronous during coherent motion, causing suppression of firing. **a**, Schematic proposal for the inputs to an OMS ganglion cell: excitation from motion in the receptive field centre, and inhibition from motion in the periphery. Both consist of transient events and are triggered by the same motion features. Under coherent motion they coincide in time, but under incoherent motion they are uncorrelated. **b**, Average firing rate of Fast OFF ganglion cells (GCs) as the jitter trajectories of the object and background regions are shifted in time relative to each other (thick red line). Firing rates were averaged over 5-min stimulus presentations, normalized to the cell's average firing rate under the Object Only condition, then averaged over five neurons. Average membrane potential of polyaxonal amacrine cells ($AC V_m$) during global (Eye Only) jitter, as a function of time before or after a ganglion cell spike in the Object Only condition using the same trajectory (thin blue line). Each amacrine cell's membrane potential was normalized by subtracting its mean and dividing by its standard deviation, which was 4 ± 1 mV (mean \pm s.e.m.; $n = 3$); note inverted axis, depolarization is downward. **c**, Membrane potential of a polyaxonal amacrine cell in response to coherent motion (top; Eye Only condition). Spiking response of a salamander Fast OFF cell to motion in the Object Only condition, using the same trajectory as for the amacrine cell (bottom). The amacrine and ganglion cells were recorded in different retinas. **d**, Vertical projection of the confocal image of the amacrine cell in **c**, superimposed on its receptive field (left). Receptive field of the ganglion cell in **c**, on the same scale (right).

relative to the excitation and thus be ineffective. To test this idea, we used the same jitter trajectory for the object and background regions, but shifted them with respect to each other in time. As predicted, the suppressive effect was limited to a very brief time window around zero delay (Fig. 4b, thick red trace). This suggests that peripheral inhibition indeed arrives in brief pulses approximately 100 ms wide, triggered by the same motion features as the excitatory events from the centre.

We searched, using intracellular recordings in the salamander retina, for interneurons that might mediate this long-range inhibition. We encountered a type of amacrine cell that responded to coherent jitter (Eye Only) with sharp depolarizations, about 100 ms wide, often carrying action potentials (Fig. 4c). These depolarizing events in amacrine cells aligned perfectly with the excitatory inputs to OMS cells, as marked by the bursts of spikes produced in the Object Only condition (Fig. 4c). If such amacrine cells inhibit the OMS ganglion cells, this could explain the suppression of firing under coherent motion. By calculating the average amacrine cell membrane potential relative to the time of a ganglion cell spike, we predicted how this inhibition should depend on the time delay between object and background motion. Figure 4b shows that the

time course of the amacrine cell membrane potential nicely predicts the measured time course of ganglion cell suppression.

These amacrine cells had visual receptive fields of about 150 μm radius (Fig. 4d), probably mediated by inputs on a small field of dendrites near the soma²¹ (see Supplementary Fig. S1). Several long output processes extended >1 mm across the retina (Fig. 4d). A ganglion cell collecting inhibitory input from these amacrine cell processes will be suppressed whenever the motion in the distant periphery matches the motion over the ganglion cell's receptive field centre. Thus both the anatomy and the physiology of these amacrine cells are consistent with their being the source of inhibition onto OMS cells. Amacrine cells with a similar polyaxonal morphology are found in other species including rabbit^{22,23} and macaque^{24,25}.

Object motion selectivity is independent of spatial pattern

For a neuron to be selective for object motion under natural viewing conditions, the timing of the excitation and inhibition should ideally depend only on the motion trajectory, and be largely independent of the spatial pattern of the stimulus. To test this we changed both the spatial phase and frequency of the object grating, while keeping the background uniformly grey. Indeed, the time

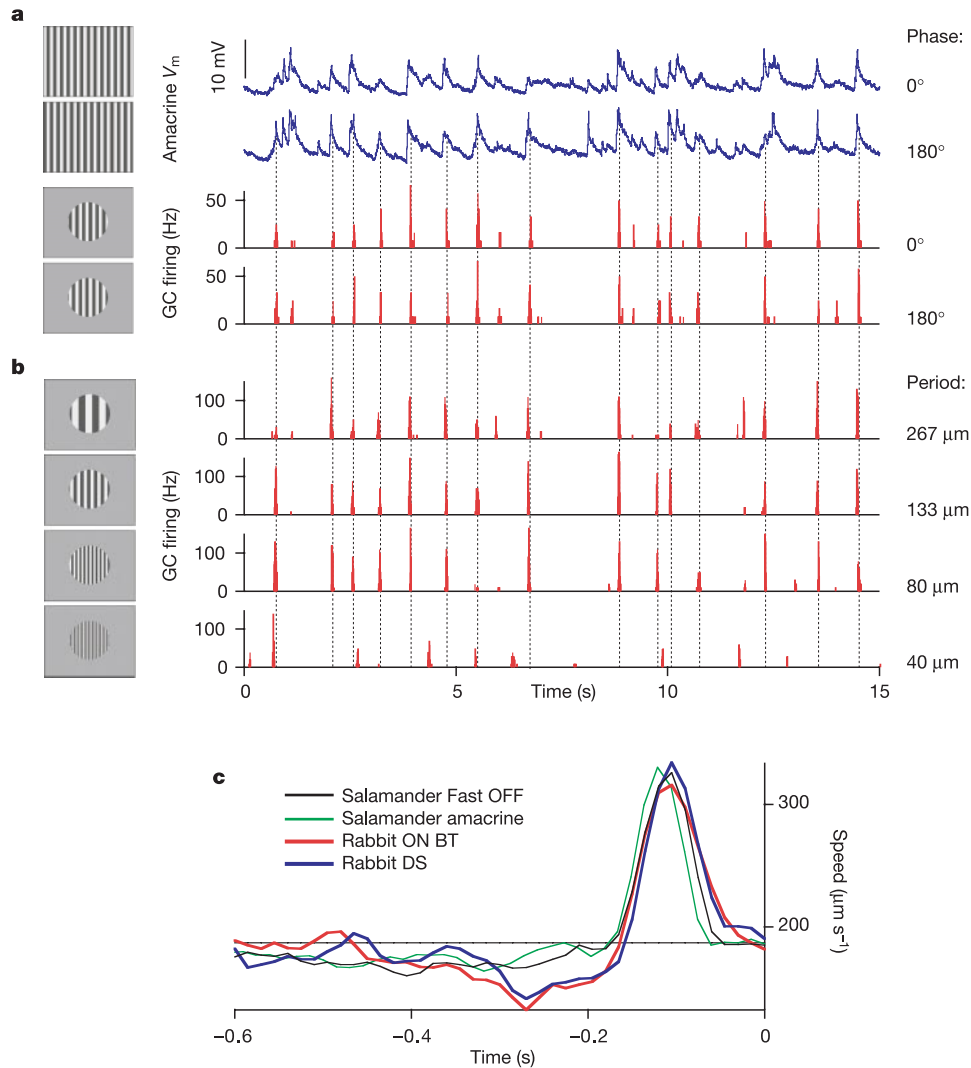


Figure 5 The response of OMS cells is largely independent of the spatial pattern. **a**, Responses of a salamander polyaxonal amacrine cell (top) and a Fast OFF ganglion cell (bottom) to a jittering grating (0°) and its contrast-reversed version (180°). **b**, Responses of a different Fast OFF ganglion cell to a grating of varying spatial period. **c**, The average time course of the retinal speed of the jittered grating before a spike for a salamander

polyaxonal amacrine cell (Eye Only condition) and three different types of OMS cells (Object Only condition): the Fast OFF cell in salamander, and the ON Brisk Transient and ON-OFF Direction Selective cells in rabbit. The time-averaged speed for the entire stimulus is marked by the horizontal line.

course of firing of OMS cells did not depend on the spatial phase of the grating: even a 180° phase shift, corresponding to a complete reversal of black and white bars, did not significantly alter the cell's response (Fig. 5a). Nor did such a phase reversal alter the response of polyaxonal amacrine cells (Fig. 5a). Varying the spatial frequency of the grating also had little effect on the firing pattern of the ganglion cells (Fig. 5b), except for very fine gratings with period <40 μm. In that limit, the firing rate declined and the spike bursts were triggered at different time points in the motion trajectory. Polyaxonal amacrine cell responses were similarly robust to changes in spatial frequency (data not shown). These properties differed from those of other amacrine cell types. For example, the responses of sustained OFF-type amacrine cells to coherent motion (Eye Only) were uncorrelated with the excitatory inputs to OMS ganglion cells, and strongly depended on the phase and spatial frequency of the jittered grating (Supplementary Fig. S2).

Whereas the response of OMS cells is largely independent of the spatial pattern, it is almost completely determined by the motion trajectory (Fig. 5a, b). We calculated the average image speed before a spike for three types of OMS cells, and for salamander polyaxonal amacrine cells, in response to a jittered object. The average motion feature that triggered spikes was an acceleration of the grating after a period of slower than average speed (Fig. 5c). For most OMS cells this stimulus was effective regardless of the direction of motion; however, the rabbit ON-OFF Direction Selective cell responded only when the grating accelerated in its preferred direction.

Increasing or decreasing the speed of the jitter by a factor of two did not significantly alter the shape of the preferred speed profile; neither did it alter the OMS cells' sensitivity to differential motion (not shown). This suggests that the function of OMS cells is robust to changes in the statistics of eye movements, which accompany changes in the behavioural state of the animal^{7,26}. Note also that the preferred motion feature for the polyaxonal amacrine cell is

remarkably similar to that which excites the receptive field centres of OMS ganglion cells. This suggests that an inhibitory network involving a single type of amacrine cell could serve to suppress different types of OMS ganglion cells in the same retina.

A model explaining object motion selectivity

The fact that these cells respond to gratings much finer than the receptive field centre, and independently of the phase of the grating, is reminiscent of the Y-type ganglion cells found in cat²⁷ and many other mammals. It is thought that the Y-cell pools excitation from many small subunits in its receptive field, each of which contributes a rectified response²⁸. We implemented a concrete version of this idea (Fig. 6a) and simulated how it would respond to the jittered grating stimulus in the Object Only condition. With just two free parameters, this simple model reproduced with good accuracy the timing of ganglion cell firing in both salamander and rabbit retina (Fig. 6b).

The model's response is independent of the direction of motion and the phase of the grating, because the receptive field centre contains subunits arranged symmetrically in all directions and at all possible phases relative to the grating. Similarly, the response is largely independent of spatial frequency, as long as the bars of the grating are larger than the subunit width. When the stripes become smaller, the model's output declines, and a comparison to the observed responses (Fig. 5b) suggests a minimum subunit width of 20–40 μm. It has been proposed that bipolar cells form the nonlinear subunits of ganglion cell receptive fields^{29,30}. We recorded intracellularly from bipolar cells in the salamander retina. Their receptive field centres measured 35–120 μm (*n* = 7) in width (data not shown), in agreement with the dendritic field size of salamander bipolar cells³¹, and consistent with their role as nonlinear subunits.

The model in Fig. 6a includes an inhibitory network that pools over many nonlinear subunits in the periphery. The fact that the excitatory and inhibitory networks receive input from the same type of subunits results in a selectivity for differential motion between

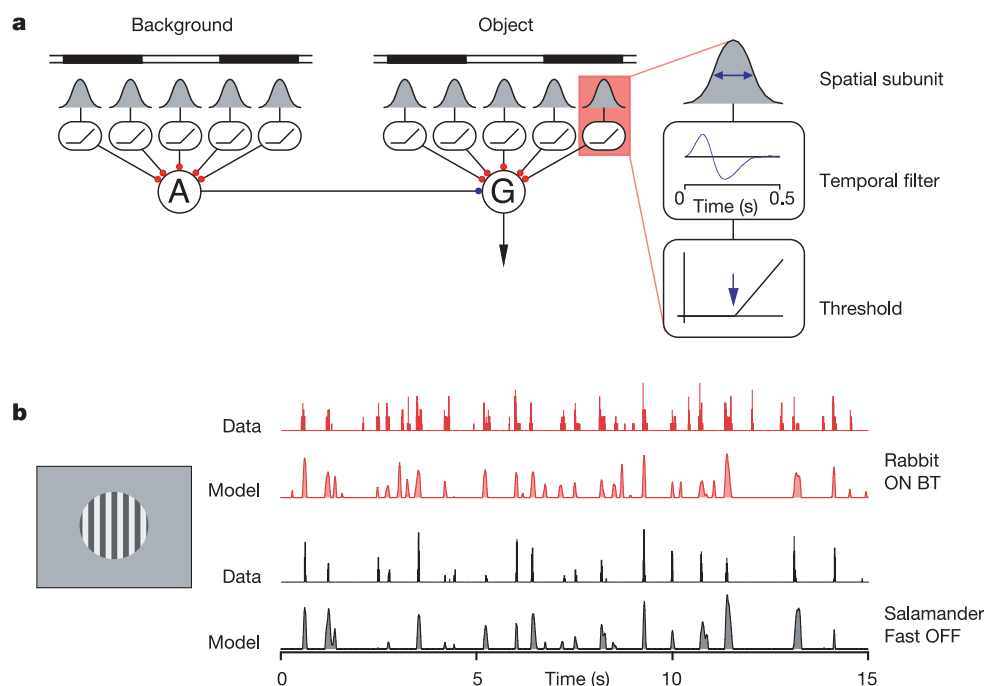


Figure 6 A model of retinal processing that accounts for differential motion sensitivity. **a**, The OMS ganglion cell (G) receives additive excitatory input from many nonlinear subunits underlying the object region. It is also inhibited by amacrine cells (A) that pool over similar nonlinear subunits underlying the background. Each subunit (right) pools light

over a small receptive field, passes the result through a temporal filter, and rectifies the result above a threshold (arrow). **b**, Simulated responses to a jittered grating using the model in **a**, compared to the responses of real OMS cells to the same jitter (see Methods). The stimulus trajectory was the same for both salamander and rabbit cells.

the receptive field centre and the surround. This is accomplished without explicitly computing and comparing the motion vectors in the two regions, contrary to what was found for motion contrast sensors in higher visual centres¹⁵. In fact, the behaviour of this model is not in any way dependent on the direction of motion, only on the speed. To test this prediction, we performed an experiment in which the object and background regions jittered with exactly opposite trajectories, and found that the recorded responses from OMS cells were indeed suppressed, just as under the coherent motion condition (Supplementary Fig. S3). Although this situation represents a departure from the ideal of differential motion detection, it rarely arises in nature, because the relative motion of an object within the scene would have to mimic the observer's eye movements.

Among the rabbit Brisk Transient cells, only the ON-type is suppressed by global motion (Fig. 2e); presumably the OFF-type receives different inhibitory input. For the purpose of detecting object motion it is not essential to have OMS properties in both ON- and OFF-type Brisk Transient cells. Owing to the nonlinear spatial summation, the model of Fig. 6a predicts that an OMS cell would have the same response to a moving pattern whether its subunits are ON-type or OFF-type. This prediction was confirmed experimentally, as the rabbit ON-type OMS cell and the salamander OFF-type OMS cell fired at similar times during the motion trajectory (see Figs 2a–d, 5c and 6b).

Motion pop-out and binding

Finally, we consider how a population of OMS cells represents a visual scene composed of several objects. For this, the stimulus included two objects moving with different trajectories on an incoherently jittering background (Fig. 7a). We recorded the response of many Fast OFF ganglion cells in the salamander retina at more than 200 positions relative to the stimulus display. Figure 7b shows a map of the firing rate in this population. In the region covered by the two moving objects, ganglion cells fired vigorously. In the background region, the cells were suppressed, because they experienced coherent motion between their receptive field centres and the wider periphery. Thus, a population of OMS cells could

support the perceptual ‘motion pop-out’ effect, which flags local motion within the scene and attracts our visual attention. This pop-out would involve only a short delay: in salamander, the median spike latency of these cells from the onset of object motion was about 230 ms (data not shown).

Sudden movement of an image on the retina is known to synchronize firing in multiple ganglion cells³². Inspection of the spike trains in the two-object experiment showed that OMS cells covering the same object indeed fired in synchrony (Fig. 7c, d), whereas OMS cells seeing differently moving objects were uncorrelated (Fig. 7d). This is expected from the model of Fig. 6a, as the receptive field centres of cells covering the same object experience the same trajectory, and consequently the same speed time course. Because the firing responses are sparse, two neurons belonging to differently moving objects will only rarely fire together by chance. Thus, a group of OMS cells with persistent coincident activity can define a moving object, regardless of its visual pattern or its exact motion trajectory. Segregation of objects based on motion cues is a well-described perceptual phenomenon³³. It has been suggested that synchronous firing is the tag that ‘binds’ neurons together in an assembly to represent a visual object³⁴. The circuitry of Fig. 6a is a candidate for the underlying neural mechanism.

Discussion

Our experiments involved the retinas of rabbit and salamander, but the essential building blocks required for OMS cells are present in many other species, including primates. Approximately 20% of the magnocellular ganglion cells in the primate retina show nonlinear spatial summation similar to that of our model (Fig. 6a)^{35–37}. Transient, polyaxonal amacrine cells as in Fig. 4d with narrow dendritic and receptive fields and large axonal arborizations have also been found in the macaque retina^{4,25}. Thus, it is probable that ganglion cells with OMS properties exist in many species, including humans. These cells serve as an information channel for object motion and may support diverse functions such as segregating object from background, and directing the gaze towards moving targets.

One would predict that inadvertent stimulation of OMS neurons

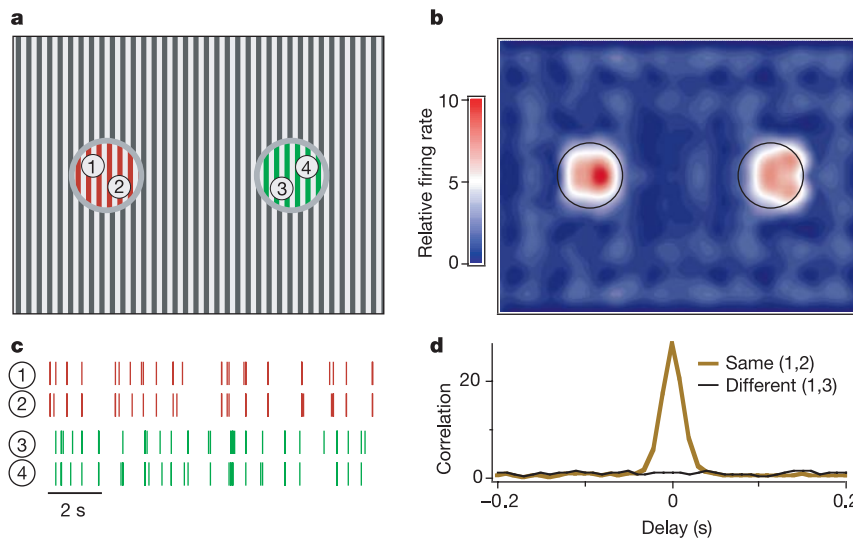


Figure 7 Pop-out of moving objects in a population of OMS ganglion cells. **a**, Schematic of the stimulus: two object regions (red and green, each 800 μm in diameter) are moving with different trajectories on an incoherently jittering background. Encircled numbers denote the receptive field positions of the cells in **c**. **b**, Map of the firing rate in a population of salamander Fast OFF ganglion cells responding to the stimulus in **a** (see Methods).

c, Segment of the spike trains from two pairs of cells covering two differently moving objects: 1 and 2 respond to the object on the left (red), whereas 3 and 4 respond to the object on the right (green). **d**, Cross-correlation function between the spike trains of two cells responding to either the same object (1,2; thick brown line), or differently moving objects (1,3; thin line), normalized by the product of the two cells' mean firing rates.

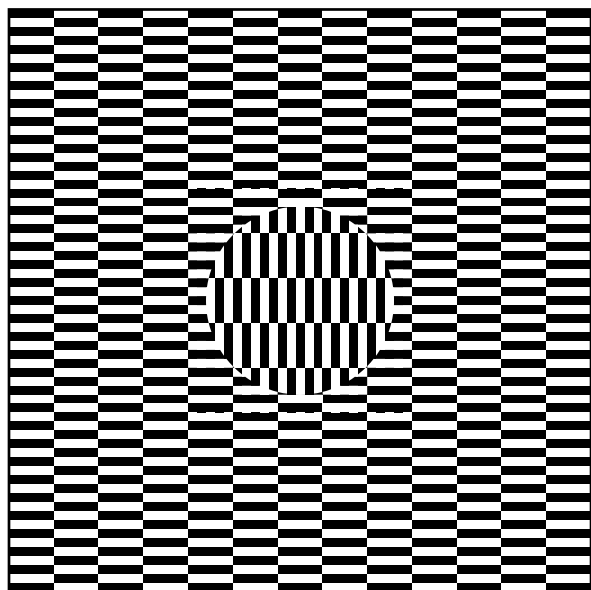


Figure 8 A motion illusion revealed by the Japanese artist Ouchi³⁸. The circle appears to float and jitter relative to the background.

should evoke an erroneous perception of object motion. We propose that this happens when viewing certain geometrical patterns, such as the Ouchi illusion³⁸ (Fig. 8). Owing to the unusual geometry of the display, retinal motion of the pattern is mainly governed by vertical eye movements in the periphery, and by horizontal eye movements in the centre. Because the eye executes horizontal and vertical eye movements independently⁵, centre and periphery experience different image motion—analogue to the Eye + Object stimulus (Fig. 2a). This triggers the OMS cells to signal an apparent movement of the circle. Although this is an example of a spatial pattern influencing the response of OMS cells, it should be noted that the geometric peculiarities required for this effect are rare in the natural environment, where retinal function evolved.

We have shown that certain retinal ganglion cells with nonlinear spatial summation have a special role in the presence of fixational eye movements: such a neuron signals when an object in its receptive field centre moves relative to the background, but is almost completely suppressed when the object moves together with the background. This selectivity for object motion in any direction is accomplished by a rather simple mechanism with three crucial ingredients: excitation from many rectified subunits in the receptive field centre; inhibition from the same type of subunits in a wide surround; and the random nature of fixational eye movements that produces transient and sparse activation of both the excitatory and inhibitory networks. □

Methods

Recordings

Retinas of larval tiger salamanders, and Dutch belted and New Zealand white rabbits were isolated in darkness and superfused with oxygenated Ringer's medium at room temperature (salamander) or Ames' solution at 36 °C (rabbit). A piece of retina, 6–8 mm on a side, was placed with the ganglion cell layer facing down on a multi-electrode array, which recorded spike trains simultaneously from many ganglion cells, as described previously³⁹. For intracellular recordings from salamander⁴⁰, sharp microelectrodes were filled with 2 M potassium acetate and 4% neurobiotin, having a final impedance of 150–250 MΩ. Polyaxonal amacrine cell resting membrane potentials ranged from –50 to –75 mV, and their peak responses to jittered gratings were 17 ± 4 mV (mean \pm s.e.m.; $n = 7$) in amplitude. To analyse amacrine cell spiking (Fig. 5c), the action potentials were detected by setting a threshold for the derivative of the membrane potential. After recording, cells were filled iontophoretically (1–5 nA pulses, about 10–15 min), stained with $5 \mu\text{g ml}^{-1}$ streptavidin Alexa-488 (Molecular Probes), and imaged using a confocal microscope with a $\times 40$ oil immersion objective.

Stimulation

Visual stimuli were projected from a computer monitor onto the photoreceptor layer, as described³⁹. All experiments used a mean photopic intensity of 8 mW m^{-2} . Unless otherwise stated, the jittered grating consisted of black and white bars with a periodicity of $133 \mu\text{m}$. The jitter trajectory was generated by stepping the grating randomly in one dimension every 15 ms with a step size of $6.7 \mu\text{m}$. The seeds for generating the random walk in the object and background regions were the same or different for the Eye Only and Eye + Object conditions, respectively. The object region, $800 \mu\text{m}$ in diameter, was separated from the background region, measuring $4,300 \times 3,200 \mu\text{m}$, by a $67\text{-}\mu\text{m}$ grey annulus, except for the experiment in Fig. 3a, where no annulus was present. For Fig. 3b the stimulus was a spot of varying size flashing from black to white at 1 Hz on a grey background. In experiments with different stimulus conditions, the trials were interleaved.

Receptive field mapping

The spatio-temporal receptive fields of all neurons were measured by reverse correlation to a flickering black-and-white checkerboard stimulus³⁹. The spatio-temporal receptive field was approximated as the product of a spatial profile and a temporal filter. The receptive field centre of a ganglion cell was estimated as the region where the spatial profile was larger than one-third of its maximum value. The diameter of the receptive field centre of amacrine and bipolar cells was approximated by the full-width at half-maximum of the two-dimensional gaussian function that best fit the spatial profile.

Cell types

Retinal ganglion cells appear in distinct functional types. For salamander, we classified them on the basis of their spatio-temporal receptive fields⁴¹. We report on the responses of the Fast OFF (~60% of recorded cells), Weak OFF (~12%) and ON cells (~12%). Rabbit ganglion cells were classified on the basis of the spatio-temporal receptive field and the spike train's autocorrelation function, following the criteria of ref. 42. For rabbit, we report on data from ON–OFF Direction Selective cells (~30% of recorded cells), OFF Brisk Transient cells (~20%), ON Brisk Transient cells (~15%) and Local Edge Detectors (~15%). Other cell types in rabbit were encountered rarely, and are not reported.

Analysis

Only ganglion cells with receptive field centres enclosed by the object region were included in the analyses, except for Fig. 3, where only cells with receptive fields concentric with the object region were included. Error bars in figures denote standard error, derived from variation among cells. For calculating the average speed profiles in Fig. 5c, the jitter trajectory was smoothed using a 30-ms box filter. During the experiments for Fig. 7b, the object regions were shifted in increments of $530 \mu\text{m}$ along both the horizontal and vertical dimensions. Responses from 11 salamander Fast OFF cells were analysed, each sampled at 20 independent positions of the stimulus. Each cell's firing rate was normalized with respect to its firing rate under the Eye Only condition. In Fig. 7b, the image value at a given point is the average normalized firing rate of all cells whose receptive field centre contained that point. The results were mirrored on the axis of symmetry in the stimulus, and smoothed using a two-dimensional gaussian filter (standard deviation of $70 \mu\text{m}$).

Simulation

For the simulations in Fig. 6, the subunit width (full width at half maximum of a parabolic profile) was chosen as $42 \mu\text{m}$ for both salamander and rabbit, within the measured range of bipolar cell receptive fields; simulations were robust to changes in this parameter. The waveform of the temporal filter was measured by reverse correlation of ganglion cell spikes to a flicker stimulus⁴³. The threshold was set so that the subunit outputs were non-zero 2.5% (salamander) or 3.5% (rabbit) of the time. The subunits were centred $6.7 \mu\text{m}$ apart, effectively sampling all possible phases relative to the stimulus grating. The region covered by the excitatory subunits was chosen larger than one grating period.

Received 20 December 2002; accepted 18 March 2003; doi:10.1038/nature01652.
Published online 11 May 2003.

1. Yarbus, A. L. *Eye Movements and Vision* (Plenum, New York, 1967).
2. Kowler, E. *Eye Movements and their Role in Visual and Cognitive Processes* (Elsevier, New York, 1990).
3. Ross, J., Morrone, M. C., Goldberg, M. E. & Burr, D. C. Changes in visual perception at the time of saccades. *Trends Neurosci.* **24**, 113–121 (2001).
4. Coppola, D. & Purves, D. The extraordinarily rapid disappearance of entopic images. *Proc. Natl Acad. Sci. USA* **93**, 8001–8004 (1996).
5. Skavenski, A. A., Hansen, R. M., Steinman, R. M. & Winterson, B. J. Quality of retinal image stabilization during small natural and artificial body rotations in man. *Vision Res.* **19**, 675–683 (1979).
6. Manteuffel, G., Plasa, L., Sommer, T. J. & Wess, O. Involuntary eye movements in salamanders. *Naturwissenschaften* **64**, 533–534 (1977).
7. Van der Steen, J. & Collewijn, H. Ocular stability in the horizontal, frontal and sagittal planes in the rabbit. *Exp. Brain Res.* **56**, 263–274 (1984).
8. Gibson, J. J. *The Perception of the Visual World* (Houghton Mifflin, Boston, 1950).
9. Vernon, M. D. *The Psychology of Perception* (Penguin, Baltimore, Maryland, 1962).
10. Graham, C. H. in *Vision and Visual Perception* (ed. Graham, C. H.) 575–588 (Wiley, New York, 1965).
11. Hammond, P. & Smith, A. T. On the sensitivity of complex cells in feline striate cortex to relative motion. *Exp. Brain Res.* **47**, 457–460 (1982).
12. Born, R. T. & Tootell, R. B. Segregation of global and local motion processing in primate middle temporal visual area. *Nature* **357**, 497–499 (1992).
13. Bender, D. B. & Davidson, R. M. Global visual processing in the monkey superior colliculus. *Brain Res.* **381**, 372–375 (1986).
14. Sterling, P. & Wickelgren, B. G. Visual receptive fields in the superior colliculus of the cat. *J. Neurophysiol.* **32**, 1–15 (1969).
15. Frost, B. J. & Nakayama, K. Single visual neurons code opposing motion independent of direction. *Science* **220**, 744–745 (1983).

16. Steinman, R. M. & Collewijn, H. Binocular retinal image motion during active head rotation. *Vision Res.* **20**, 415–429 (1980).
17. Cook, P. B., Lukasiewicz, P. D. & McReynolds, J. S. Action potentials are required for the lateral transmission of glycinergic transient inhibition in the amphibian retina. *J. Neurosci.* **18**, 2301–2308 (1998).
18. Werblin, F. S. Lateral interactions at inner plexiform layer of vertebrate retina: antagonistic responses to change. *Science* **175**, 1008–1010 (1972).
19. Enroth-Cugell, C. & Jakiela, H. G. Suppression of cat retinal ganglion cell responses by moving patterns. *J. Physiol.* **302**, 49–72 (1980).
20. Passaglia, C. L., Enroth-Cugell, C. & Troy, J. B. Effects of remote stimulation on the mean firing rate of cat retinal ganglion cells. *J. Neurosci.* **21**, 5794–5803 (2001).
21. Werblin, F., Maguire, G., Lukasiewicz, P., Eliasof, S. & Wu, S. M. Neural interactions mediating the detection of motion in the retina of the tiger salamander. *Visual Neurosci.* **1**, 317–329 (1988).
22. Famiglietti, E. V. Polyaxonal amacrine cells of rabbit retina: size and distribution of PA1 cells. *J. Comp. Neurol.* **316**, 406–421 (1992).
23. Volgyi, B., Xin, D., Amarillo, Y. & Bloomfield, S. A. Morphology and physiology of the polyaxonal amacrine cells in the rabbit retina. *J. Comp. Neurol.* **440**, 109–125 (2001).
24. Dacey, D. M. Axon-bearing amacrine cells of the macaque monkey retina. *J. Comp. Neurol.* **284**, 275–293 (1989).
25. Stafford, D. K. & Dacey, D. M. Physiology of the A1 amacrine: a spiking, axon-bearing interneuron of the macaque monkey retina. *Vis. Neurosci.* **14**, 507–522 (1997).
26. Grossman, G. E., Leigh, R. J., Bruce, E. N., Huebner, W. P. & Lanska, D. J. Performance of the human vestibuloocular reflex during locomotion. *J. Neurophysiol.* **62**, 264–272 (1989).
27. Hochstein, S. & Shapley, R. M. Linear and nonlinear spatial subunits in Y cat retinal ganglion cells. *J. Physiol.* **262**, 265–284 (1976).
28. Shapley, R. M. & Victor, J. D. Nonlinear spatial summation and the contrast gain control of cat retinal ganglion cells. *J. Physiol.* **290**, 141–161 (1979).
29. Victor, J. D. & Shapley, R. M. The nonlinear pathway of Y ganglion cells in the cat retina. *J. Gen. Physiol.* **74**, 671–689 (1979).
30. Demb, J. B., Zaghloul, K., Haarsma, L. & Sterling, P. Bipolar cells contribute to nonlinear spatial summation in the brisk-transient (Y) ganglion cell in mammalian retina. *J. Neurosci.* **21**, 7447–7454 (2001).
31. Wu, S. M., Gao, F. & Maple, B. R. Functional architecture of synapses in the inner retina: segregation of visual signals by stratification of bipolar cell axon terminals. *J. Neurosci.* **20**, 4462–4470 (2000).
32. Greschner, M., Bongard, M., Rujan, P. & Ammermuller, J. Retinal ganglion cell synchronization by fixational eye movements improves feature estimation. *Nature Neurosci.* **5**, 341–347 (2002).
33. Regan, D. *Human Perception of Objects: Early Visual Processing of Spatial Form Defined by Luminance, Color, Texture, Motion, and Binocular Disparity* (Sinauer, Sunderland, Massachusetts, 2000).
34. Singer, W. Neuronal synchrony: a versatile code for the definition of relations? *Neuron* **24**, 49–65 (1999).
35. Blakemore, C. & Vital-Durand, F. Organization and post-natal development of the monkey's lateral geniculate nucleus. *J. Physiol.* **380**, 453–491 (1986).
36. Kaplan, E. & Shapley, R. M. The primate retina contains two types of ganglion cells, with high and low contrast sensitivity. *Proc. Natl Acad. Sci. USA* **83**, 2755–2757 (1986).
37. Shapley, R., Kaplan, E. & Soodak, R. Spatial summation and contrast sensitivity of X and Y cells in the lateral geniculate nucleus of the macaque. *Nature* **292**, 543–545 (1981).
38. Ouchi, H. *Japanese Optical and Geometrical Art* (Dover, New York, 1977).
39. Meister, M., Pine, J. & Baylor, D. A. Multi-neuronal signals from the retina: acquisition and analysis. *J. Neurosci. Methods* **51**, 95–106 (1994).
40. Baccus, S. A. & Meister, M. Fast and slow contrast adaptation in retinal circuitry. *Neuron* **36**, 909–919 (2002).
41. Warland, D. K., Reinagel, P. & Meister, M. Decoding visual information from a population of retinal ganglion cells. *J. Neurophysiol.* **78**, 2336–2350 (1997).
42. DeVries, S. H. Correlated firing in rabbit retinal ganglion cells. *J. Neurophysiol.* **81**, 908–920 (1999).
43. Chichilnisky, E. J. A simple white noise analysis of neuronal light responses. *Network* **12**, 199–213 (2001).

Supplementary Information accompanies the paper on www.nature.com/nature.

Acknowledgements We thank members of the Meister laboratory for advice; P. Cavanagh, F. Engert, V. Murthy and K. Nakayama for comments on the manuscript; and H. van der Steen for providing the eye movement data in Fig. 1b. This work was supported by a grant from NEI (M.M.) and NRSA (S.A.B.).

Competing interests statement The authors declare that they have no competing financial interests.

Correspondence and requests for materials should be addressed to M.M. (meister@fas.harvard.edu).